Quantum interference in spontaneous emission of an atom embedded in a double-band photonic crystal

Han Zhuang Zhang,* Sing Hai Tang, Po Dong, and Jun He
Department of Physics, National University of Singapore, Singapore 117542, Singapore

(Received 15 October 2001; revised manuscript received 22 January 2002; published 29 May 2002)

Quantum interferences in spontaneous emission spectrum from a V-type three-level and a double V-type four-level atom embedded in a double-band photonic band-gap material have been investigated. We demonstrate that there is not only a black dark line, but also a narrow spontaneous line in the spectrum. The dark line results from a destructive interference or singularities of the density of states of the radiation field. The narrow spectral line arises from a population transfer under joint constructive interferences. The spontaneous emission spectrum is compared to the cases of single-band and double-band photonic band-gap reservoirs.

DOI: 10.1103/PhysRevA.65.063802 PACS number(s): 42.50.Gy, 42.70.Qs

I. INTRODUCTION

It is generally envisaged that narrowing down the spontaneous emission and dark lines will lead to a multitude of potential applications in high-precision measurements, lasing without inversion, quantum computation, teleportation, and quantum information theory. For this purpose, a multilevel atom coupled by the same vacuum mode and additionally driven by coherent laser fields is widely studied. The interference effects in such a system lead to many remarkable phenomena, including very narrow absorption and fluorescence spectra [1–6], population trapping in a degenerate system [7,8], fluorescence quenching in the free space [4,9,10], phase dependent line shapes [11,12], lasing without inversion [13], and others.

It is well known that spontaneous emission depends not only on the energy structure of an atom but also on the nature of the surrounding environment, more specifically, on the density of states (DOS) of the radiation field [14,15]. In recent years, photonic band-gap (PBG) structures have been shown to have different DOS in comparison with the free-space vacuum field [14–17]. The study of quantum and nonlinear optical phenomena for atoms embedded in such PBG materials leads to the prediction of many interesting effects, for example, localization of light [18,19], photon-atom bound states [14,15,18,20], suppression and even complete cancellation of spontaneous emission [21,22], enhancement of spontaneous emission [23–26], electromagnetically induced transparency, and other phenomena [27–32].

When the V-type three-level atom is coupled to the vacuum space reservoir without external driving field, the quantum interference between decay processes from the two upper levels to a lower level can result in a dark line in the spontaneous emission spectrum, as reported by Zhu [1]. It leads us to pose the next question: if a similar atomic system were coupled with a PBG reservoir rather than with the vacuum space reservoir, what would be the resulting spontaneous emission spectrum near the edges of the photonic band? As far as we know, Zhu and co-workers [23–26] had studied the electric-field components in spontaneous emission from an atom with a V-type energy diagram embedded in a photonic crystal. While the spontaneous emission spectrum near the photonic band edge has been mentioned in a few papers [31,32], the discussions are limited to population involution and distribution of the upper levels based on a single-band PBG reservoir. In contrast, we focus in this paper on the spontaneous emission spectrum, rather than the population involution and distribution, and consider the V-type three-level atom as well as a double V-type four-level atom embedded in a double-band photonic crystal described by both isotropic and anisotropic dispersion relations at the band edges.

Most interestingly, it is shown that in addition to the expected dark line an extremely narrow spontaneous line near the transition from the empty upper level to a lower level may be produced. These properties may be used to amplify a laser field with narrow linewidth without population inversion. In practical realization of controlling and suppressing spontaneous emission, the system of atoms embedded in a double-band photonic crystal in this paper is, in fact, experimentally more versatile than another system of atoms coupled to a free vacuum field. This is due to the fact that the width of the band gap can be tailor designed to the levels of an atom in the fabrication of the photonic crystal. For example, with the parameters chosen in this paper, the difference between the atomic levels and the edges of the forbidden gap can be matched for best lasing interaction. In Sec. II, we derive the equations for describing the spontaneous emission spectrum of the three-level atom. The resulting quantum interference from a V-type three-level atom in a double-band photonic crystal is presented in Sec. III. In Sec. IV we discuss the two types of quantum interferences from a double V-type four-level atom in a double-band photonic crystal. The major conclusions are summarized in Sec. V.

II. EQUATIONS FOR THE SPONTANEOUS EMISSION SPECTRUM

. We consider first a V-type three-level atom with upper levels labeled by $|3\rangle$ and $|2\rangle$, and lower level labeled by $|1\rangle$, as shown in Fig. 1 without additional dotted level $|0\rangle$. The

*Permanent address: Department of Physics, Jilin University in China.
Email address: Phyzhz@nus.edu.sg; Hzzhang@mail.jlu.edu.cn

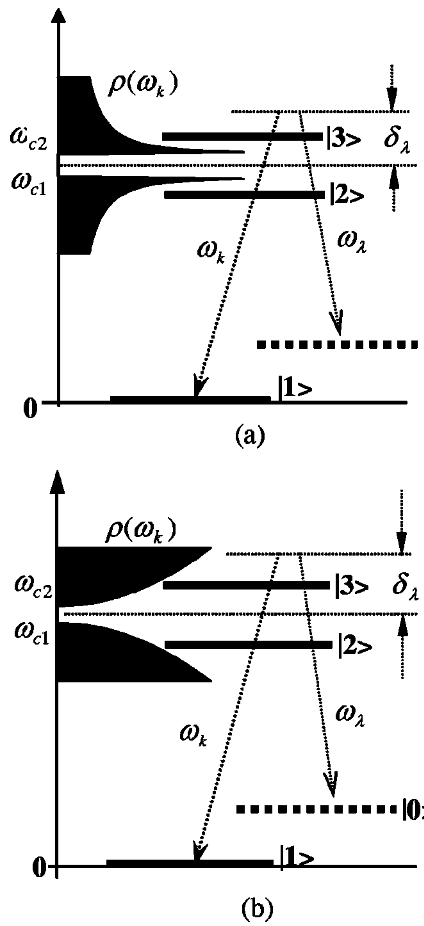

FIG. 1. Schematic diagram of an atom in a double photonic band structure. $|1\rangle$, $|2\rangle$, and $|3\rangle$ correspond to a three-level atom model. $|1\rangle$, $|2\rangle$, and $|3\rangle$ with additional level $|0\rangle$ shown as the dotted line correspond to a four-level model. $\rho(\omega_k)$ denotes the density of state of the PBG modes. ω_{c2} and ω_{c1} are the upper and lower frequencies of the forbidden gap, respectively. δ_λ is the detuning of frequency of the radiation field of the free vacuum modes from the middle of the forbidden gap. It was assumed that the transitions from the upper levels $|3\rangle$ and $|2\rangle$ to the lower level $|0\rangle$ and the level $|1\rangle$ are coupled by free vacuum modes ω_λ and PBG modes ω_k, respectively. (a) The double-band isotropic PBG reservoir. (b) The double-band anisotropic PBG reservoir.

transitions from the two upper levels to the lower level can be coupled by the double-band isotropic PBG reservoir as shown in Fig. 1(a), or by the anisotropic PBG reservoir as shown in Fig. 1(b). The dispersion relations near the photonic band edges are approximated by [14]

$$\omega_k=\omega_{c1}-A_1(k-k_0)^2,\quad k<k_0,$$

$$\omega_k=\omega_{c2}+A_2(k-k_0)^2,\quad k>k_0, \tag{1}$$

$$\omega_k=\omega_{c1}-A_1|(\vec{k}-\vec{k}_0)|^2,\quad |\vec{k}|<|\vec{k}_0|,$$

$$\omega_k=\omega_{c2}+A_2|(\vec{k}-\vec{k}_0)|^2,\quad |\vec{k}|>|\vec{k}_0| \tag{2}$$

for isotropic dispersion relation and anisotropic dispersion relation, respectively, where $A_n\approx\omega_{cn}/k_0^2$ $(n=1,2)$, ω_{c1} and ω_{c2} are the upper and lower frequencies at the edges of the forbidden gap, respectively. The Hamiltonian describing the dynamics of this system in the interaction picture and the rotating wave approximation can be written as

$$H_i=i\hbar\sum_{k\lambda}\,(g_{k\lambda}^{31}a_{k\lambda}^\dagger b_1^\dagger b_3 e^{i\mu_k^{31}t}+g_{k\lambda}^{21}a_{k\lambda}^\dagger b_1^\dagger b_2 e^{i\mu_k^{21}t}-\text{c.c.}), \tag{3}$$

where $g_{k\lambda}^{j1}$ $(j=2,3)$ is the frequency-dependent coupling constant between the atomic transition $|j\rangle$-$|1\rangle$ and the mode $\{k\lambda\}$ of the radiation field. More precisely,

$$g_{k\lambda}^{j1}=\frac{\omega_{j1}d_{j1}}{\hbar}\left(\frac{\hbar}{2\varepsilon_0\omega_k V}\right)^{1/2}\vec{e}_{k\lambda}\cdot\vec{d}_{j1},$$

$$\mu_k^{j1}=\omega_k-\omega_{j1}\quad (j=2,3); \tag{4}$$

here $\vec{d}_{j1}$ $(j=2,3)$ is the atomic dipole moment unit vector for the transition $|j\rangle$-$|1\rangle$, $\vec{e}_{k\lambda}$ $(\lambda=1,2)$ is the polarization unit vector of radiation field, and V is the sample volume. The state vector of the system in the interaction picture can be written as

$$|\Psi(t)\rangle=A_3(t)|3,\{0\}\rangle+A_2(t)|2,\{0\}\rangle+\sum_{k\lambda}\,A_{1k\lambda}|1,\{k\lambda\}\rangle. \tag{5}$$

Substituting Eqs. (3) and (5) into Schrodinger equation, we obtain

$$\frac{dA_3(t)}{dt}=-\sum_{k\lambda}\,g_{k\lambda}^{31}e^{-i\mu_k^{31}t}A_{1k\lambda}(t),$$

$$\frac{dA_2(t)}{dt}=-\sum_{k\lambda}\,g_{k\lambda}^{21}e^{-i\mu_k^{21}t}A_{1k\lambda}(t),$$

$$\frac{dA_{1k\lambda}(t)}{dt}=g_{k\lambda}^{31}e^{i\mu_k^{31}t}A_3(t)+g_{k\lambda}^{21}e^{i\mu_k^{21}t}A_2(t). \tag{6}$$

Formally integrating and eliminating $A_{1k\lambda}$ from Eq. (6), we get

$$\frac{dA_3(t)}{dt}=-\int_0^t G_{33}(t-t')A_3(t')dt'-e^{i\omega_{32}t}\times\int_0^t G_{32}(t-t')A_2(t')dt',$$

$$\frac{dA_2(t)}{dt}=-\int_0^t G_{22}(t-t')A_2(t')dt'-e^{-i\omega_{32}t}\times\int_0^t G_{23}(t-t')A_3(t')dt', \tag{7}$$

where

$$G_{jl}(t-t')=\sum_{k\lambda}\,g_{k\lambda}^{j1}g_{k\lambda}^{l1}\exp[-i\mu_k^{l1}(t-t')]\quad (j,l=2,3) \tag{8}$$

is the delay Green's function that can be expressed in the following forms [14]:

$$G_{jl}(t-t')=\eta_{jl}\frac{1}{2}\sqrt{\beta_{j1}^{3/2}\beta_{l1}^{3/2}}\left(\frac{\exp\{i[\delta_{l1c2}(t-t')-\pi/4]\}}{\sqrt{\pi(t-t')}}+\frac{\exp\{i[\delta_{l1c1}(t-t')+\pi/4]\}}{\sqrt{\pi(t-t')}}\right),$$

$$G_{jl}(t-t')=\eta_{jl}\frac{1}{2}\sqrt{\alpha_{j1}\alpha_{l1}}\left(\frac{\exp\{i[\delta_{l1c2}(t-t')+\pi/4]\}}{\sqrt{4\pi(t-t')^3}}+\frac{\exp\{i[\delta_{l1c1}(t-t')-\pi/4]\}}{\sqrt{4\pi(t-t')^3}}\right),$$

$$G_{jl}(t-t')=\eta_{jl}\frac{1}{2}\sqrt{\gamma_{j1}\gamma_{l1}}\delta(t-t') \tag{9}$$

for isotropic PBG, anisotropic PBG, and free-space reservoirs, respectively. The definitions of the parameters are [14]

$$\beta_{j1}^{3/2}=\frac{1}{2\pi\varepsilon_0}\frac{\omega_{j1}^2 d_{j1}^2\omega_{c2}^{3/2}}{3\hbar c^3},$$

$$\alpha_{j1}=\frac{1}{2\pi\varepsilon_0}\frac{\omega_{j1}^2 d_{j1}^2\omega_{c2}^{1/2}}{3\hbar c^3},$$

$$\gamma_{j1}=\frac{2}{\pi\varepsilon_0}\frac{\omega_{j1}^3 d_{j1}^2}{3\hbar c^3}. \tag{10}$$

Here β_{j1} and α_{j1}^2 are the resonant frequency splittings [18], γ_{j1} effective decay rate for the transition from the upper level j ($j=2{,}3$) to a lower level. β_{j1}, α_{j1}^2, and γ_{j1} have the same dimension of inversed second [14]. In Eq. (9), $\eta_{jl}=\delta_{jl}+\eta(1-\delta_{jl})$ ($j,l=2{,}3$) and both δ_{jl} and δ are the delta functions. $\eta=(3/8\pi)\int(\cos\varphi_{31}\cos\varphi_{21}+\cos\upsilon_{31}\cos\upsilon_{21})d\Omega$, where $\{\varphi_{j1},\upsilon_{j1},\theta_{j1}\}$ ($j=2{,}3$) are the directional angles of the dipole moment unit vector $\vec{d}_{j1}$ in a coordinate system defined by the unit vectors $\{\vec{e}_{k1},\vec{e}_{k2},\vec{k}\}$, and $d\Omega$ is the solid angle. So $\eta=1.0$ when $\vec{d}_{j1}\cdot\vec{d}_{l1}=\pm 1$, and $\eta=0$ when $\vec{d}_{j1}\cdot\vec{d}_{l1}=0$; otherwise, $0<\eta<1.0$. The parameters $\eta_{22}=\eta_{33}=1.0$ are independent of η. The parameter η_{32} is the coupling coefficient between the transitions from the two upper levels to the lower level. When the dipole moments of the two transitions are orthogonal, $\eta_{32}=0$, implying that there is no quantum interference between the two transitions. When the dipole moments of the two transitions are parallel or antiparallel, $\eta_{32}=1.0$, implying that the quantum interference is maximal between the two transitions. Therefore, η_{32} is an effective measure of quantum interference.

The spontaneous spectrum of the atom, $S(\omega_k)$, is the Fourier transform of [1]

$$\langle E^-(t+\tau)E^+(t)\rangle_{t\to\infty}=\langle\Psi(t)|\sum_{k,k'}a_k^\dagger a_{k'}e^{i\omega_k(t+\tau)}e^{-i\omega_{k'}t}|\Psi(t)\rangle_{t\to\infty}. \tag{11}$$

Substituting Eq. (5) into Eq. (11), we have

$$\langle E^-(t+\tau)E^+(t)\rangle_{t\to\infty}=\sum_{k\lambda}A_{1k\lambda}^*(\infty)A_{1k\lambda}(\infty)e^{i\omega_k\tau}=\int_{-\infty}^{+\infty}e^{i\omega_k\tau}d\omega_k D(\omega_k)\int\sum_{\lambda=1}^{2}A_{1k\lambda}^*(\infty)A_{1k\lambda}(\infty), \tag{12}$$

where $D(\omega_k)$ is the DOS of the radiation field, which can be derived as [14]

$$D(\omega_k)\sim\frac{1.0}{\sqrt{\omega_k-\omega_{c2}}}\Theta(\omega_k-\omega_{c2})+\frac{1.0}{\sqrt{\omega_{c1}-\omega_k}}\Theta(\omega_{c1}-\omega_k),$$

$$D(\omega_k)\sim\sqrt{\omega_k-\omega_{c2}}\Theta(\omega_k-\omega_{c2})+\sqrt{\omega_{c1}-\omega_k}\Theta(\omega_{c1}-\omega_k),$$

$$D(\omega_k)\sim 1.0, \tag{13}$$

for isotropic PBG, anisotropic PBG, and free-space reservoirs, respectively, where Θ is the Heaviside step function. From Eqs. (4), (6), (10), and (12), we have

$$\begin{aligned}S(\omega_k)\sim D(\omega_k)[&p_{k31}^2\tilde{A}_3^*(s)_{s\to-i\mu_k^{31}}\tilde{A}_3(s)_{s\to-i\mu_k^{31}}\\&+p_{k21}^2\tilde{A}_2^*(s)_{s\to-i\mu_k^{21}}\tilde{A}_2(s)_{s\to-i\mu_k^{21}}\\&+\eta_{32}p_{k31}p_{k21}\{\tilde{A}_3^*(s)_{s\to-i\mu_k^{31}}\tilde{A}_2(s)_{s\to-i\mu_k^{21}}\\&+\tilde{A}_2^*(s)_{s\to-i\mu_k^{21}}\tilde{A}_3(s)_{s\to-i\mu_k^{31}}\}],\end{aligned} \tag{14}$$

where the definitions of $p_{kj1}(j=2{,}3)$ are

$$p_{kj1}=\sqrt{\beta_{j1}^{3/2}},$$

$$p_{kj1}=\sqrt{\alpha_{j1}},$$

$$p_{kj1}=\sqrt{\gamma_{j1}}, \tag{15}$$

for isotropic PBG, anisotropic PBG, and free-space reservoirs, respectively, and $\tilde{A}_j(s)(j=2{,}3)$ is the Laplace transform of $A_j(t)$. Taking the Laplace transform of Eq. (7), we obtain

$$\tilde{A}_3(s)_{s\rightarrow -i\mu_k^{31}}=\frac{[-i\mu_k^{21}+\tilde{G}_{22}(-i\mu_k^{21})]A_3(0)-\tilde{G}_{32}(-i\mu_k^{21})A_2(0)}{[-i\mu_k^{31}+\tilde{G}_{33}(-i\mu_k^{31})][-i\mu_k^{21}+\tilde{G}_{22}(-i\mu_k^{21})]-\tilde{G}_{32}(-i\mu_k^{31})\tilde{G}_{32}(-i\mu_k^{21})},$$

$$\tilde{A}_2(s)_{s\rightarrow -i\mu_k^{21}}=\frac{[-i\mu_k^{31}+\tilde{G}_{33}(-i\mu_k^{31})]A_2(0)-\tilde{G}_{23}(-i\mu_k^{31})A_3(0)}{[-i\mu_k^{31}+\tilde{G}_{33}(-i\mu_k^{31})][-i\mu_k^{21}+\tilde{G}_{22}(-i\mu_k^{21})]-\tilde{G}_{32}(-i\mu_k^{31})\tilde{G}_{32}(-i\mu_k^{21})}, \tag{16}$$

where $\omega_{32}=\omega_{31}-\omega_{21}$ is the frequency difference of the upper two levels, $A_2(0)$ and $A_3(0)$ are the initial values of $A_2(t)$ and $A_3(t)$, and $\tilde{G}_{jl}(s)$ is the Laplace transform of the delay Green's function in Eq. (8), which can be derived in the forms of

$$G_{jl}(s\rightarrow -iu_k^{l_1})=\eta_{jl}\frac{1}{2}\sqrt{\beta_{j1}^{3/2}\beta_{l1}^{3/2}}\left\{\frac{i}{\sqrt{\mu_k^{l1}+\delta_{l1c1}}}+\frac{1.0}{\sqrt{\mu_k^{l1}+\delta_{l1c2}}}\right\},$$

$$G_{jl}(s\rightarrow -iu_k^{l_1})=\eta_{jl}\frac{1}{2}\sqrt{\alpha_{j1}\alpha_{l1}}\{-i\sqrt{\mu_k^{l1}+\delta_{l1c1}}+\sqrt{\mu_k^{l1}+\delta_{l1c2}}\},$$

$$G_{jl}(s\rightarrow -iu_k^{l_1})=\eta_{jl}\frac{1}{2}\sqrt{\gamma_{j1}\gamma_{l1}}\quad (j,l=2,3) \tag{17}$$

for isotropic PBG, anisotropic PBG, and free-space reservoirs, respectively. Here the definitions of the detuning parameters are

$$\mu_k^{21}=\mu_k^{31}+\omega_{32}=\mu_k^{31}+\delta_{31c2}+\delta_{c2c1}-\delta_{21c1},$$

$$\delta_{31c1}=\delta_{31c2}+\delta_{c2c1},$$

$$\delta_{21c2}=\delta_{21c1}-\delta_{c2c1},$$

$$\delta_{31c2}=\omega_{31}-\omega_{c2},$$

$$\delta_{21c1}=\omega_{21}-\omega_{c1}, \tag{18}$$

where δ_{j1cl} is the difference between the upper level j ($j=2,3$) and the lower edge ($l=1$) or the upper edge ($l=2$) of the forbidden gap. We assume that the radiation-field reservoir is initially in the vacuum state, and the atom is prepared in a coherent superposition of the upper levels $|3\rangle$ and $|2\rangle$ in the form of

$$|\Psi(0)\rangle=\cos(\theta)|3\{0\}\rangle+\sin(\theta)e^{i\Delta\phi}|2\{0\}\rangle. \tag{19}$$

Comparing Eqs. (5) and (19), we obtain

$$A_3(0)=\cos(\theta),$$

$$A_2(0)=\sin(\theta)e^{i\Delta\phi},$$

$$A_{1k\lambda}(0)=0, \tag{20}$$

where $\Delta\phi$ and θ are, respectively the initial phase difference between the two upper-level states and the mixing angle of the initial populations. The calculation of spontaneous emission spectrum can be performed based on Eqs. (14), (16), (13), (17), and the parameters defined in Eqs. (15), (18), and (20). It is seen that the parameter η_{32} is embodied not only in the third term, but also in the first and second terms on the right side of Eq. (14). Therefore, quantum interference exhibits itself in all the terms on the right side of Eq. (14). This is different from the case studied in Ref. [1] where quantum interference is included only in the cross term [see Eq. (13) in Ref. [1]]. The interesting features resulting from the interference are discussed in the following sections.

III. THE QUANTUM INTERFERENCE FROM A V-TYPE THREE-LEVEL ATOM IN A DOUBLE-BAND PBG

A. A narrow spectral line resulting from quantum interference

We study first the case where an atom is equally and synchronously pumped to the upper levels. In Figs. 2(a)–2(c), the spontaneous emission spectra are shown for the cases of isotropic PBG reservoir, anisotropic PBG reservoir, and free-space vacuum reservoir, respectively. Here, symmetric values of parameters for the two transitions are employed (i.e., the same detunings $\delta_{31c2}=-\delta_{21c1}=1.0$, and the same coupling constants $\beta_{31}=\beta_{21}=1.0$, $\alpha_{31}^2=\alpha_{21}^2=1.0$, $\gamma_{31}=\gamma_{21}=1.0$). Figure 2 shows that while quantum interference leads to a dark line in the spectrum in the case of a free-space vacuum reservoir as discussed by Zhu [1], it has relatively weaker effects on the spontaneous emission spectrum in the cases of isotropic and anisotropic PBG reservoirs. In order to compare the quantum interference of the three-level atom in the PBG reservoir to that in the vacuum space reservoir [1], we assume that the atom is initially pumped to level $|3\rangle$. Asymmetric parameters of the two atomic transitions are chosen to have similar values to those of Ref. [1]. However, the ensuing emissions are quite different. Figure 3 shows the spectral features of the quantum interference. In Fig. 3(c), we see as expected that the quantum interference induces a dark line in the spectrum at around the frequency of the transition from $|2\rangle$ to $|1\rangle$ and an attempt to build a peak near the dark line position in the case of free-space vacuum reservoir, as discussed in detail by Zhu. However, for the cases of the isotropic PBG reservoir [Fig. 3(a)] and anisotropic PBG reservoir [Fig. 3(b)], we see that not only does the dark line persist to exist, but also the attempt to build a peak as mentioned earlier in Fig. 3(c) is strongly enhanced into a very narrow spectral line whose position is near the frequency of the transition from the empty upper level $|2\rangle$ to the lower level $|1\rangle$.

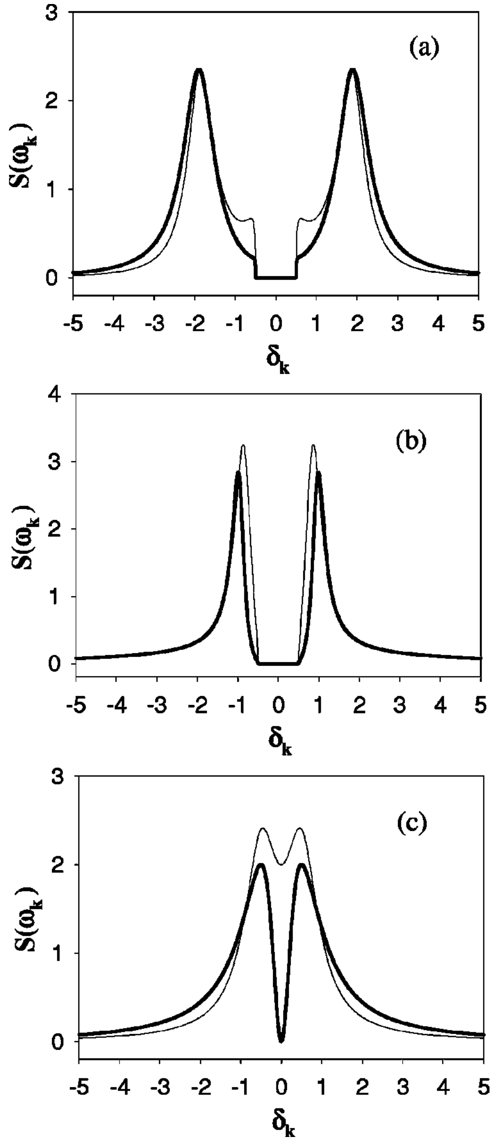

FIG. 2. The spontaneous emission spectrum $S(\omega_k)$ (in arbitrary units) as a function of detuning δ_k. (a) Double-band isotropic PBG reservoir and $\beta_{21}=1.0$, (b) double-band anisotropic PBG reservoir and $\alpha_{21}^2=1.0$, (c) free vacuum reservoir and $\omega_{32}=1.0$, $\gamma_{21}=1.0$. The other parameters used are $\theta=0.25$, $\Delta\phi=0$, $\delta_{c2c1}=1.0$, $\delta_{31c2}=1.0$, $\delta_{21c1}=-1.0$, and $\eta_{32}=0$ (for thin lines), $\eta_{32}=1.0$ (for thick lines). All parameters are in units of β_{31}, α_{31}^2, and γ_{31} for isotropic PBG modes, anisotropic PBG modes, and free vacuum modes, respectively, except that θ and $\Delta\phi$ are in units of π and η_{32} is dimensionless

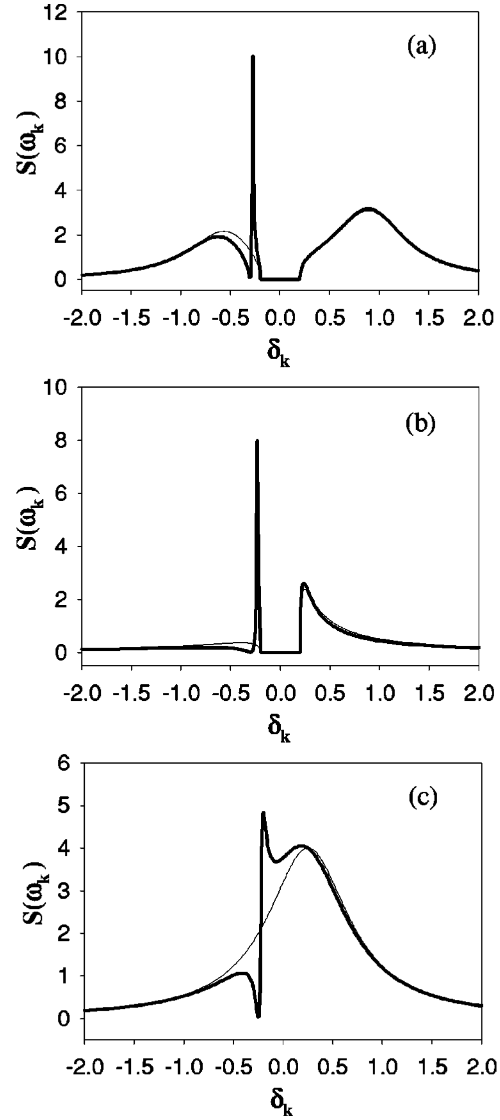

FIG. 3. The spontaneous emission spectrum $S(\omega_k)$ (in arbitrary units) as a function of detuning δ_k. (a) Double-band isotropic PBG reservoir and $\beta_{21}=0.1$, (b) double-band anisotropic PBG reservoir and $\alpha_{21}^2=0.1$, (c) free vacuum reservoir and $\omega_{32}=0.5$, $\gamma_{21}=0.1$. The other parameters used are $\theta=0$, $\Delta\phi=0$, $\delta_{c2c1}=0.4$, $\delta_{31c2}=0.1$, $\delta_{21c1}=-0.1$, $\eta_{32}=0$ (for thin lines), $\eta_{32}=1.0$ (for thick lines)

The appearance of the narrow line could not possibly stem from cutting off by the gap in the PGB case. This can be seen from Fig. 4, which shows that when both of the upper levels are located in the same band and far from the edges of photonic band, the narrow spontaneous line still persists. It is well known that quantum interference, which may be destructive or constructive [4], can induce a population transfer between the two upper levels [14]. Here, the dark line results from destructive interference, and the narrow spectral line arises from a population transfer under constructive interference. The fact that the bright narrow spontaneous line can be realized in the PBG structure but not in the free space stems from the difference in the DOS of the radiation field.

B. The difference in the spontaneous emission spectrum between double-band and single-band PBG reservoir

In this section, we consider the spontaneous emission spectra of the same atom embedded in a single-band PBG material and compare the results with those in the double-band PBG material described previously. In order to compare, we assume that in both cases the two upper levels are located in the upper band. The spontaneous emission spectra are shown in Fig. 4 for the case of the isotropic [Fig. 4(a)] and anisotropic [Fig. 4(b)] PBG reservoirs, and the two cases of single-band (thin solid lines) and double-band (thick solid

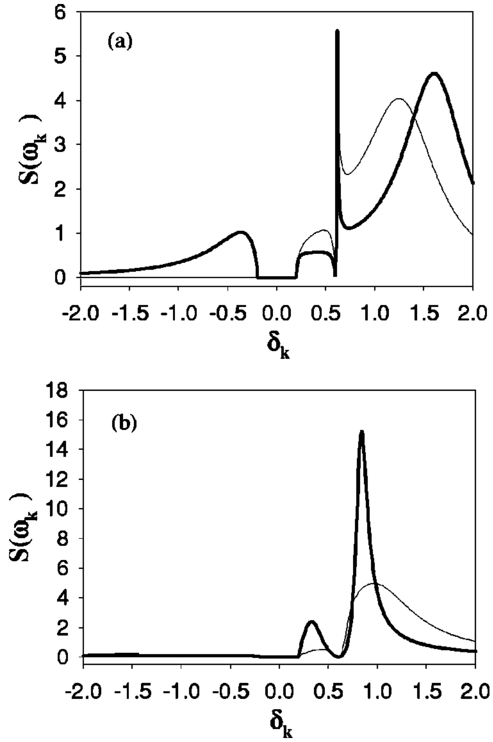

FIG. 4. The spontaneous emission spectrum $S(\omega_k)$ (in arbitrary units) as a function of detuning δ_k for a one-band PBG reservoir (thin lines) and a double-band PBG reservoir (thick lines). (a) Isotropic PBG reservoir and $\beta_{21}=0.1$. (b) Anisotropic PBG reservoir and $\alpha_{21}^2=0.1$. The other parameters used are $\theta=0$, $\Delta\phi=0$, $\eta_{32}=1.0$, $\delta_{c2c1}=0.4$, $\delta_{31c2}=1.0$, $\delta_{21c1}=0.8$ (for double band) and $\delta_{21c2}=0.4$ (for single band).

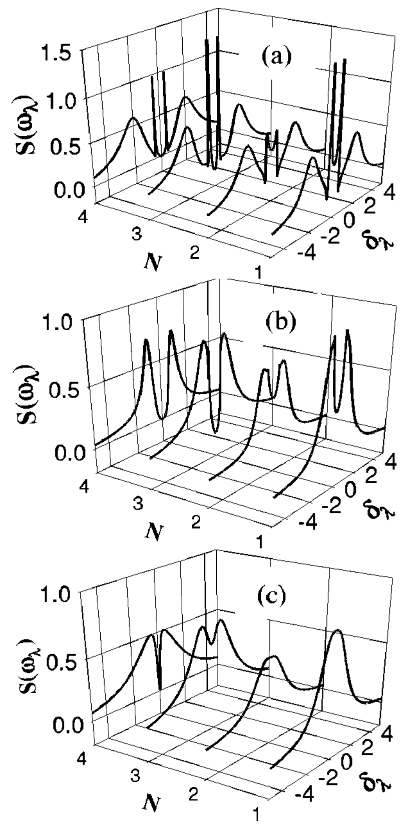

FIG. 5. The spontaneous emission spectrum $S(\omega_\lambda)$ (in arbitrary units) as a function of detuning δ_λ for different coherent coupling constants. The plots at the positions $N=1$, 2, 3, 4 correspond to $(\eta_{32}^\lambda=0,\eta_{32}^k=0)$, $(\eta_{32}^\lambda=0,\eta_{32}^k=1)$, $(\eta_{32}^\lambda=1,\eta_{32}^k=0)$, and $(\eta_{32}^\lambda=1,\eta_{32}^k=1)$, respectively. (a) For the double-band isotropic PBG reservoir and $\beta_{31}=\beta_{20}=\gamma_{21}=1.0$. (b) For the double-band anisotropic PBG reservoir and $\alpha_{31}^2=\alpha_{20}^2=\gamma_{21}=1.0$. (c) For the free vacuum reservoir and $\omega_{32}=1.0$, $\gamma_{31}=\gamma_{20}=\gamma_{21}=1.0$. The other parameters used are $\theta=0.25$, $\Delta\phi=0$, $\delta_{c2c1}=1.0$, $\delta_{31c2}=1.0$, $\delta_{21c1}=-1.0$. All parameters are in units of γ_{31} except that θ and $\Delta\phi$ are in units of π, and η_{32}^λ and η_{32}^k are dimensionless.

lines). From Fig. 4, we see that when both of the upper levels are located in the same band, the width of the spectral line remains narrow in the case of the isotropic PBG reservoir, while it becomes larger in the case of the anisotropic PBG reservoir. Most interestingly, we see that the width of the spontaneous emission line can be manipulated, larger or narrower, in the case of the double-band PBG reservoir as compared with that of the single-band PBG reservoir.

IV. THE TWO TYPES OF QUANTUM INTERFERENCES FROM A DOUBLE V-TYPE FOUR-LEVEL ATOM IN A DOUBLE-BAND PBG

In the preceding section, both transitions from the upper levels to the common lower level are coupled to the same non-Markov environment. Consequently, there is only one possible quantum interference in this V-type three-level model. For the case of Λ-type three-level model as discussed by Knight and his co-workers [28], the transitions from the common upper level to the two lower levels interact independently with free vacuum modes and PBG modes. It is obvious that there is no quantum interference in this model. However, based on the Λ-type three-level model, a double V-type four-level model can be constructed with a double V-type transitions, as shown in Fig. 1 with additional dotted level $|0\rangle$. In this model, the transitions from the two upper levels to the two lower levels $|0\rangle$ and $|1\rangle$ are coupled, respectively, by the free vacuum modes and PBG modes as in the Λ-type three-level model, leading to two possible types of quantum interferences. The first is ascribed to atomic transitions coupled to the PBG modes, and the second arises from atomic transitions coupled to the free vacuum modes. As far as we know, there are no reports on the effects of the two types of quantum interference on the spontaneous emission spectrum for the case of transitions from the upper levels to the lower level $|0\rangle$ coupled to the free vacuum modes. Following the sequence of the preceeding section, we study first the case where an atom is equally and synchronously pumped to the upper levels. In Figs. 5(a)–5(c), the spontaneous emission spectra are shown for the cases of the transitions $|3\rangle$-$|1\rangle$ and $|2\rangle$-$|1\rangle$ coupled to the isotropic PBG reservoir, anisotropic PBG reservoir, and free-space vacuum reservoir, respectively. Here, symmetric values of parameters (i.e., same detunings $\delta_{31c2}=-\delta_{21c1}=1.0$, same coupling constants $\beta_{31}=\beta_{21}=1.0$, $\alpha_{31}^2=\alpha_{21}^2=1.0$, $\gamma_{31}=\gamma_{21}=1.0$, and $\gamma_{30}=\gamma_{20}=1.0$) for the double V-type structure are employed. The plots at the positions $N=1$, 2, 3, 4 correspond to $(\eta_{32}^\lambda$

$=0, \eta_{32}^{k}=0)$, $(\eta_{32}^{\lambda}=0, \eta_{32}^{k}=1)$, $(\eta_{32}^{\lambda}=1, \eta_{32}^{k}=0)$, and $(\eta_{32}^{\lambda}=1, \eta_{32}^{k}=1)$, respectively. Figure 5 shows that altogether three dark lines appear in the case of the isotropic PBG reservoir [Fig. 5(a)], but there exists only one dark line in the cases of the anisotropic PBG [Fig. 5(b)] or free vacuum reservoir [Fig. 5(c)]. From Fig. 5, we also see that the dark lines at the center of $\delta_{\lambda}=0$ in all three cases coincide with those reported by Zhu [1], and hence they are due to the quantum interference of the transitions between $|3\rangle$-$|0|\rangle$ and $|2\rangle$-$|0\rangle$. The two dark lines at symmetric sides of $\delta_{\lambda}=0$ in Fig. 5(a) originate from the two singularities in the Laplace transform of the delay Green's function, as shown in Eq. (13), which is equivalent to the DOS of the isotropic PBG modes. It is seen that the interference between the transitions $|3\rangle$-$|1\rangle$ and $|2\rangle$-$|1\rangle$ has a rather weak effect on the spontaneous spectrum in this case. However, the situation is quite different if the atom is assumed to be initially pumped to level $|3\rangle$ and some other values for the parameters of the double V-type model are employed. New features resulting from the two types of quantum interferences are shown in Fig. 6. While the dark lines persist to exist, a new narrow spontaneous line has emerged in all three cases. The narrow line is attributed to the transition from the upper level $|2\rangle$ with empty population to the lower level $|0\rangle$. The dark lines are consequences of destructive interference between the transitions $|3\rangle$-$|0\rangle$ and $|2\rangle$-$|0\rangle$, or singularities of the radiation field's DOS similar to that mentioned previously in the V-type three-level model. In contrast, quantum interferences arising from the transitions coupled to free vacuum modes alone is unable to induce the narrow spontaneous line ($N=3$ in Fig. 6). It is a resultant of ($N=4$ in Fig. 6) constructive interferences of the double V-type transitions coupled, respectively, to the free vacuum modes and the PBG modes, producing simultaneously a population transfer between the two upper levels.

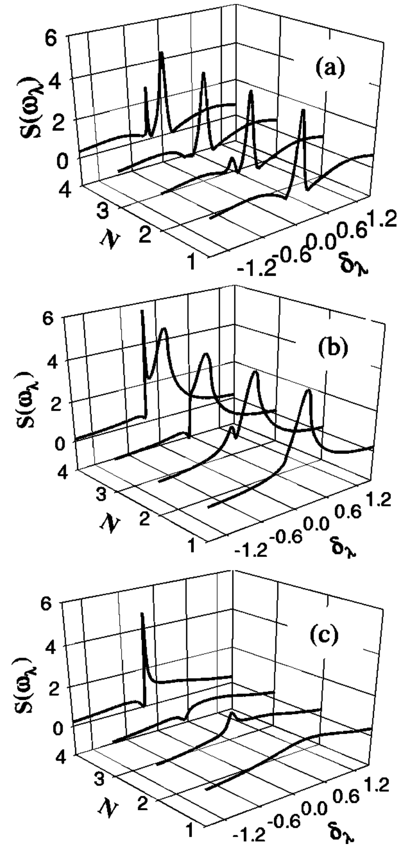

FIG. 6. The spontaneous emission spectrum $S(\omega_{\lambda})$ (in arbitrary units) as a function of detuning δ_{λ} for different coherent coupling constants. The plots at the positions $N=1$, 2, 3, 4 correspond to $(\eta_{32}^{\lambda}=0, \eta_{32}^{k}=0)$, $(\eta_{32}^{\lambda}=0, \eta_{32}^{k}=1)$, $(\eta_{32}^{\lambda}=1, \eta_{32}^{k}=0)$, and $(\eta_{32}^{\lambda}=1, \eta_{32}^{k}=1)$, respectively. (a) For the double-band isotropic PBG reservoir and $\beta_{31}=1.0$, $\beta_{20}=\gamma_{21}=0.1$. (b) For the double-band anisotropic PBG reservoir and $\alpha_{31}^{2}=1.0$, $\alpha_{20}^{2}=\gamma_{21}=0.1$. (c) For the free vacuum reservoir and $\omega_{32}=0.5$, $\gamma_{31}=1.0$, $\gamma_{20}=\gamma_{21}=0.1$. The other parameters used are $\theta=0$, $\Delta\phi=0$, $\delta_{c2c1}=0.4$, $\delta_{31c2}=0.1$, $\delta_{21c1}=-0.1$.

V. CONCLUSION

Summarizing, the spontaneous emission spectra of V-type and double V-type atoms embedded in a double-band photonic crystal have been investigated. Most interestingly it is shown that in a V-type three-level model only one type of quantum interference gives rise to not only a dark line, but also an extremely narrow spontaneous line in the spectrum. While there are two possible quantum interferences in a double V-type four-level model, it is seen that neither one alone can induce a narrow spontaneous line. It is rather a consequence of collective quantum interferences of the double V-type transitions coupled to free vacuum modes and PBG modes. The narrow emission line and dark lines are near the transitions from the upper levels with empty population to the lower level. The quantum interference, which may be destructive or constructive, can induce a population transfer between the two upper levels. Therefore, the dark lines result from destructive interference or singularities of the radiation field's DOS, and the narrow emission line arises from a population transfer under joint constructive interferences. The narrow spontaneous line can also be further enhanced and narrowed down in the case of double-band PBG reservoir as compared with that of single-band PBG reservoir.

[1] S. Y. Zhu, Phys. Rev. A **52**, 710 (1995).
[2] P. Zhou and S. Swain, Phys. Rev. Lett. **77**, 3995 (1996).
[3] C. H. Keitel, Phys. Rev. Lett. **83**, 1307 (1999).
[4] S. Y. Zhu and M. O. Scully, Phys. Rev. Lett. **76**, 388 (1996).
[5] P. Zhou and S. Swain, Phys. Rev. A **56**, 3011 (1997).
[6] P. Zhou and S. Swain, Phys. Rev. Lett. **78**, 832 (1997).
[7] G. S. Agarwal, *Quantum Optics*, Springer Tracts in Modern Physics Vol. 70 (Springer, Berlin, 1974).
[8] P. M. Radmore and P. L. Knight, J. Phys. B **15**, 561 (1982).
[9] H. Lee, P. Polynkin, M. O. Scully, and S. Y. Zhu, Phys. Rev. A **55**, 4454 (1997).
[10] P. R. Berman, Phys. Rev. A **58**, 4886 (1998).

[11] E. Paspalakis and P. L. Knight, Phys. Rev. Lett. **81**, 293 (1998).

[12] E. Paspalakis, N. J. Kylstra, and P. L. Knight, Phys. Rev. Lett. **82**, 2079 (1999).

[13] M. O. Scully, S. Y. Zhu, and A. Gavrielides, Phys. Rev. Lett. **62**, 2813 (1989).

[14] M. Woldeyohannes and S. John, Phys. Rev. A **60**, 5046 (1999).

[15] P. Lambropoulos, G. M. Nikolopoulos, T. R. Nielsen, and S. Bat, Rep. Prog. Phys. **63**, 455 (2000).

[16] E. Yablonovitch, Phys. Rev. Lett. **58**, 2059 (1987).

[17] S. John, Phys. Rev. Lett. **58**, 2486 (1987).

[18] S. John and T. Quang, Phys. Rev. A **50**, 1764 (1994).

[19] S. John and J. Wang, Phys. Rev. B **43**, 12 772 (1991).

[20] G. M. Nikolopoulos and P. Lambropoulos, Phys. Rev. A **61**, 053812 (2000).

[21] A. G. Kofman, G. Kurizki, and B. Sherman, J. Mod. Opt. **41**, 353 (1994).

[22] S. Bay, P. Lambropoulos, and K. Molmer, Phys. Rev. A, **55**, 1485 (1997).

[23] S. Y. Zhu, H. Chen, and H. Huang, Phys. Rev. Lett. **79**, 205 (1997).

[24] Y. P. Yang and S. Y. Zhu, Phys. Rev. A **61**, 043809 (2000).

[25] Y. P. Yang and S. Y. Zhu, J. Mod. Opt. **47**, 1513 (2000).

[26] S. Y. Zhu, Y. P. Yang, H. Chen, H. Zheng, and M. S. Zubairy, Phys. Rev. Lett. **84**, 2136 (2000).

[27] E. Paspalakis, N. J. Kylstra, and P. L. Knight, Phys. Rev. A **60**, R33 (1999).

[28] D. G. Angelakis, E. Paspalakis, and P. L. Knight, Phys. Rev. A **64**, 013801 (2001).

[29] M. Konopka, Phys. Rev. A **60**, 4183 (1999).

[30] M. Lewenstein and K. Rzazewski, Phys. Rev. A **61**, 022105 (2000).

[31] N. Vats and S. John, Phys. Rev. A **58**, 4168 (1998).

[32] Y. P. Yang, Z. X. Lin, S. Y. Zhu, H. Chen, and W. G. Feng, Phys. Lett. A **270**, 41 (2000).